Epidemic Spreading and Digital Contact Tracing: Effects of Heterogeneous Mixing and Quarantine Failures

Abbas K. Rizi,[1] Ali Faqeeh,[1,2,3] Arash Badie-Modiri,[1] and Mikko Kivelä[1]

[1] *Department of Computer Science, School of Science, Aalto University, FI-0007, Finland*
[2] *Mathematics Applications Consortium for Science & Industry, University of Limerick, Ireland*
[3] *CNetS, School of Informatics, Computing, & Engineering, Indiana University, Bloomington, IN, USA*

(Dated: March 24, 2021)

Contact tracing via digital tracking applications installed on mobile phones is an important tool for controlling epidemic spreading. Its effectivity can be quantified by modifying the standard methodology for analyzing percolation and connectivity of contact networks. We apply this framework for networks with varying degree distribution, the number of application users and the probability of quarantine failure. Further, we include structured populations with homophily and heterophily and the possibility of degree-targeted application distribution. Our results are based on a combination of explicit simulations and mean-field analysis. They indicate that there can be major differences in the epidemic size and epidemic probabilities which are equivalent in the normal SIR processes. Further, degree heterogeneity is seen to be especially important for the epidemic threshold but not as much for the epidemic size. The probability that tracing leads to quarantines is not as important as the application adaption rate. Finally, both strong homophily and especially heterophily with regards to application adoption can be detrimental. Overall, epidemics are very sensitive to all of the parameter values we tested out, which makes the problem of estimating the effect of digital contact tracing an inherently multidimensional problem.

In a pandemic era, until effective vaccines are widely deployed, carefully timed non-pharmaceutical interventions [1] such as school closures, travel restrictions and contact tracing [2–6] are the best tools we have for curbing the pandemic. Contact tracing is an attempt to discover and isolate asymptomatic or pre-symptomatic (exposed) individuals. In the absence of herd immunity, contact tracing is a potent low-cost intervention method since it puts people into quarantine where and when the disease spread. Therefore, it can have a major role in 1) containing a pandemic by relaxing social-distancing interventions [7], 2) providing an acceptable trade-off between public health and economic objectives [8, 9], 3) developing sustainable exit strategies [10, 11], 4) identifying future outbreaks [12] and 5) reaching the 'source' of infection [13].

Thanks to the emergence of low-cost wearable health devices [14–20] and mobile software applications, digital contact tracing can now be deployed with higher precision without the problems of manual contact tracing such as the tracing being slow and labor-intensive or having human issues related to blame, fear, confusion and politics. On the other hand, wearable devices also offer continuous access to real-time physiological data which can be used to tune other non-pharmaceutical or pharmaceutical strategies. Contact tracing is albeit limited by the low adoption of contact tracing apps in the population.

In both forms — manual [3, 4, 21–29] and digital [30–32] — contact tracing has been commonly considered as an effective strategy and different empirical data sets have validated this claim in short-time population-based controlled experiments [30, 33–37]. Its real potential in heterogeneous [38–41] populations, however, is not yet clear, especially because of the homophily in app adoption and other health behavior [42, 43]. It has been reported that app adoption is correlated with people's job, age, income and nationality [44, 45]. Degree-heterogeneity in the contact network [46] can alter epidemiological properties in the form of variance in final outbreak size [47], vanishing epidemic threshold [41, 48], hierarchical spreading [49], strong finite-size effects [50] and universality classes for critical exponents [51].

To reduce the peak and total size of the epidemic, not only the number of app adoption but also its distribution is of great significance if contact tracing is done early enough in the course of the spread. Therefore, in some parameter settings, contact tracing may not be effective enough [7, 52]. To curb the epidemic, app adoption of super-spreaders [53, 54] are needed to be taken into account since it dictates the extent to which a virus spreads in a bursty, power-law fashion [55–57] especially when there is high individual-level variation in the number of secondary transmissions [49, 58, 59].

Since the World Health Organization has declared the COVID-19 outbreak as a Public Health Emergency of International Concern, network scientists have developed different approaches towards analyzing epidemic tracing and mitigation with apps. Using the toolbox of network science, different groups have investigated the effectiveness of contact tracing based on the topology and directionality of contact networks [13, 33, 60–66]. Recently, a mathematical framework aimed at understanding how homophily in health behavior shapes the dynamics of epidemics has been introduced by Burgio *et al.* [67].

In this study, we investigate the effect of varying app coverage in homogeneous and heterogeneous contact networks with and without homophily in app adoption. Further, we explore the effect of distributing the apps randomly and preferentially to high-degree nodes [60] in these scenarios. Our main focus is on the epidemic

threshold and the final size of the epidemics, therefore, we assume the dynamics of the epidemic to be governed by the simple SIR model [46]. This model can be easily mapped to a static bond-percolation problem [68, 69] so that the epidemiological properties can be measured based on the topological structure of the underlying network [46, 70–73]. The difference in the spreading framework with the app to the normal one is that the infection cannot spread further if it passes a link between two app-users (app-adopters). That is, the infection process model needs to include the memory of the type of node it is coming from. We then extend the percolation framework such that we can add memory [74, 75] to it in order to keep track of the infection path. This leads to the observation that the epidemic size is not the same as the epidemic probability anymore.

Our results are based on explicit simulations and mean-field-type calculations of the percolation problem. Our findings show that 1) number of app-users has a direct effect on the epidemic size and epidemic probability and the difference between these two observables is larger in high-degree targeting strategy, 2) epidemics can be controlled to much better in the high-degree targeting strategy, 3) even though degree-heterogeneity can strongly affect or even vanish the epidemic threshold, high-degree targeting strategy can compensate this effect and increase the threshold significantly, 4) increasing heterophily from random mixing always increases the outbreak size and lowers the epidemic threshold, 5) increasing homophily does the opposite until an optimum, that is below the maximum homophily case, is reached and 6) the probability of contact tracing succeeding in preventing further infections is not as important as the fraction of app-users, but can still have significant effects on the epidemic size and epidemic threshold.

I. MODELLING APPROACH

A. Disease model and connection to percolation

We employ a standard SIR disease model on networks with additional dynamics given by the disease interactions with the disease tracking application. In the model, an infected (I) node will infect susceptible (S) nodes it is connected to by rate β and go to the removed state (R) after time τ.

In addition, if an app-user infects another app-user, that second node will get infected but will quarantine themselves with probability p_{app}. The quarantined user will have no further connections that would spread the infection they received from the other app-user. A noteworthy deviation from a realistic spreading case here is that we do not model quarantines that would be caused by another app-user but prevent the disease spreading from through a third node.

That is, we only model the primary infection path from the other app-user causing the alarm, but do not stop possible concurrent secondary infection paths from a third node.

The SIR processes can be studied using component size distributions of networks where parts of the links are randomly removed. Thus, the epidemic threshold, epidemic probability and epidemic size can be mapped to a percolation problem [68]. The SIR spreading process in the presence of apps can be mapped to a slightly more complicated percolation problem [33, 60]. In this mapping, every infected individual, regardless of app adoption, can infect a susceptible neighbor with transmission probability $p = 1 - e^{-\beta\tau}$ [68].

Moreover, to model the quarantines by app-users one needs to delete the links between two app-users with probability p_{app}. This ensures that we ignore the infection paths that would go through two app-users when one of them is successfully quarantined. However, removing these links also removes the second app-user from the component, even though they are infected. To correct for this we need to first find the components of the network, and then extend them, by including all app-users outside of the component that are connected to another app-user (and considering the probability p that the link is kept). See Fig. 1 for an illustration of this process, which leads us to two definitions of components: normal and extended.

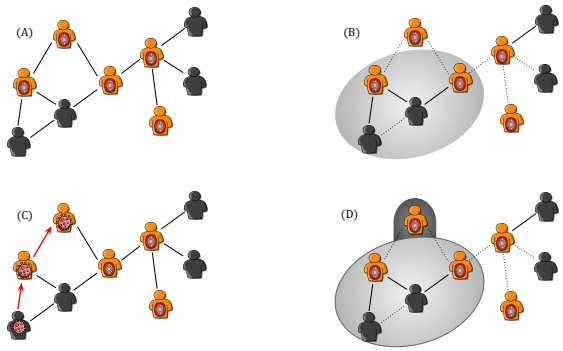

FIG. 1. (a) Original contact network with app-users marked with the oval symbol. (b) The normal largest component, after the dotted links have been removed in the percolation process by random. When apps are working perfectly, links between a pair of app-users are removed with probability $p_{\text{app}} = 1$ and other links are removed with probability p. (c) An example for a path of infection: the second app-user can be infected therefore it must be included in the outbreak size (d) Extending the giant component to include the secondary app infections. The second infected app-adapter is added to the giant component with transmission probability p.

B. Components, epidemic size and epidemic probability

In the SIR model without apps, the component size distribution can be used to fully describe the late stages

of the epidemics. Given an initially infected node, the size of the component it belongs to determines the size of the epidemic. The relationship between percolation and the final disease size is particularly simple if the population is large enough that it can be approximated with an infinite contact network. In this case, the percolation threshold gives the epidemic threshold and below it the epidemic always spans only a zero fraction of the population, because all the components are of finite size. Above the percolation threshold there is a single giant component which spans $s_{\max} = S_{\max}/N$ fraction of the nodes. This is equivalent to both the size of the epidemic, given that there is one, and the probability that there is an epidemic starting from a single initially infected node [68]. The expected size of the epidemics is in this case given as $S^2_{\max}$.

When we introduce apps to the spreading process the equivalence of the epidemic size and epidemic probability breaks down. Both the normal component and the extended component become important. The probability that there is an epidemic is still given by the component size as in the normal SIR process. However, the epidemic size, given that there is one, is now given by the extended component size $S'_{\max}$. The expected epidemic size is then given by $S_{\max}S'_{\max}$.

Similar relationships hold for finite-size systems. For example, the expected size of the epidemics from single source becomes

$$\langle E\rangle = \sum_c \frac{S_c}{N} S'_c\,, \tag{1}$$

where S_c is the normal size and S'_c is the extended size of the component c and N is the total number of nodes. In this formula, S_c/N gives the probability that the initially infected node is in the component c and S'_c gives the size of the epidemic if a node in component c is chosen.

C. Network models

We aim to study how the network topology and location of the app-users in the network affect the epidemics. We study networks with degree distribution $P(k)$ and average degree $\langle k\rangle$ such that each node is an app-user with probability $\pi_{\rm a}$ and not an app-user with probability $1-\pi_{\rm a}$. We use Poisson (ER) random graphs [76] to model homogeneous contact patterns and scale-free networks $P(k) \propto k^{-\beta}$ generated with the configuration model [46] to model heterogeneous contact patterns. The $\pi_{\rm a}N$ app-users can be picked 1) uniformly at random from the underlying network or 2) by distributing the apps in the order of their degree such that the high-degree nodes get the apps first.

To insert homophily (heterophily) in app adoption, we assume that app-users are more likely (are less likely) to be connected together. This can be controlled by the probability $\pi_{\rm aa}$ that an app-user is connected to another app-user; this stochastic block model network is a type of $\mathrm{E}^{i,i'}$ network introduced in Ref [77] with two groups of nodes: app-users and individuals without the app. The existence of homophily or heterophily of the network structure is determined by comparing $\pi_{\rm aa}$ to its value for the neutral case with no homophily or heterophily.

In the absence of homophily or heterophily, $\pi_{\rm aa} = \eta_{\rm a}$, where $\eta_{\rm a}$ is the ratio of links that emerge from app-users to the total number of stubs (nodes connections); This is because if the nodes were connected purely at random, the probability that a link from an app-user connects it to another app-user equals the ratio of the number of stubs that app-users have to the total number of stubs, i.e., $\eta_{\rm a}$. In the case of a random selection of app-users $\eta_{\rm a} = \pi_{\rm a}$, since both app-users and non-app-users have on average the same number of stubs and the fraction of stubs that app-users have equals the fraction of app-users in the system, i.e., $\pi_{\rm a}$. Nonetheless, in a high-degree targeting strategy, the number of stubs that app-users have on average is larger than that of non-app-users. In that case, $\eta_{\rm a}$ can be calculated from the degree distribution (see Sec. II B). When $\pi_{\rm aa} > \eta_{\rm a}$, app-users are more likely to be connected to each other than a purely random network in which they are connected with probability $\eta_{\rm a}$. Hence in that case there is homophily in the connection between the app-users, which means there is also homophily in the connections between non-app-users. On the other hand, when $\pi_{\rm aa} < \eta_{\rm a}$ nodes are more likely to be connected to the nodes of the other type (heterophilic network).

II. ANALYTIC AND SIMULATION METHODS

The epidemics is here studied with various levels of approximation. We employ analytical computations based on mean-field-type approximations to efficiently analyse the wide parameter space of our models and to provide explicit formulas for our main observable quantities. Here an approximation based on branching processes can be used to determine the critical point. Following Ref. [33], more detailed calculation based on percolation arguments will give us the component sizes which can be related to the final epidemic size and epidemic probability. These mean-field approximations are then complemented by simulations of the network connectivity.

A. Mean-field approximation for the branching process

An straightforward way of finding the epidemic threshold in the SIR model is to find the critical point of a branching process, where the branching factor is given by the expected excess degree q. In the epidemic setting the branching factor $R = pq$ which gives the expected number of people one infected person infects during the epidemic process. Note that this is different from the basic reproduction number that has been defined in the

networks as $R_0 = \beta/\gamma\langle k\rangle$ [69]. In the SIR model with the app, we need to duplicate the populations so that we track separately the ones without the app (S_0, I_0 and R_0) and with the app (S_A, I_A and R_A).

Given that the apps are uniformly distributed to π_a fraction of the nodes, we can write a mean-field approximation based on the branching process as follows:

$$I_0^{t+1} = (1-\pi_\mathrm{a})R(I_0^t + I_\mathrm{A}^t) \quad (2)$$
$$I_\mathrm{A}^{t+1} = \pi_\mathrm{a} R I_0^t\,, \quad (3)$$

where R is the branching factor. These equations can be rewritten as second order difference equation

$$I_0^{t+1} = (1-\pi_\mathrm{a})RI_0^t + (1-\pi_\mathrm{a})\pi_\mathrm{a}R^2 I_0^{t-1}\,. \quad (4)$$

This equation can be solved with characteristic equation, such that results is

$$I_0^t = aR_+^t + bR_-^t\,, \quad (5)$$

where a and b are constants depending on the initial conditions and R_+ and R_- are the two roots:

$$R_\pm = R\frac{1-\pi_\mathrm{a} \pm \sqrt{(1-\pi_\mathrm{a})(3\pi_\mathrm{a}+1)}}{2}\,. \quad (6)$$

For large t the larger term R_+ dominates and determines if the I_0 value will grow exponentially or decline exponentially. More precisely, there is a chance of epidemic if $R_+ > 1$. From here we can solve critical value of app-users π_a^c that are needed for reducing the reproductive number R_+ below 1 given the initial reproductive number $R > 1$:

$$\pi_\mathrm{a}^c = \frac{R-1+\sqrt{(R-1)(R+3)}}{2R}\,. \quad (7)$$

B. Giant component size from consistency equations

An alternative to the branching process approach is to form consistency equations for the giant component size. In Ref. [33] the governing equations for the size of the epidemic and the transition point were obtained for the case of random networks in the absence of homophily. Here we derive the analytical results for the more general case of the spectrum of heterophilic to homophilic networks, a special case of which are the non-homophilic networks of Ref. [33]. We consider that app-users might be connected together with a pattern different from pure random chance, this can also be the case for the non-users. In the case of a homophilic network where the app-users are more likely to be connected together, the non-users are also more likely to be connected to individuals of the same kind. This is equivalent to saying that groups of people who adopted the app are likely to be groups of nodes in the network with group members in rather close distance from each other.

To represent the bias in connection probabilities we consider that two app-users are connected with probability π_aa and other types pairs of nodes are connected with probabilities $\pi_\mathrm{an} = 1-\pi_\mathrm{aa}$, $\pi_\mathrm{na} = \frac{\pi_\mathrm{a}}{1-\pi_\mathrm{a}}(1-\pi_\mathrm{aa})$ and $\pi_\mathrm{nn} = 1-\pi_\mathrm{na} = \frac{1-\pi_\mathrm{a}-\pi_\mathrm{a}(1-\pi_\mathrm{aa})}{1-\pi_\mathrm{a}}$, where π_a and is the probability that a person is an app-user and the second equality comes from the balance between the number of links from app-users to non-app-users and from non-app to app-users, that is, $\pi_\mathrm{a}N\pi_\mathrm{an}\langle k\rangle = (1-\pi_\mathrm{a})N\pi_\mathrm{na}\langle k\rangle$.

Our aim is to write the self-consistency equations for the probability, u_0, that following a link to a non-app-user does not lead to the giant component and probability u_a, that following a link to an app-user does not lead to the giant component.

Similar to Ref. [33], we can write the conditional probabilities of u_0 and u_a given that they have degree k as

$$u_0(k) = \sum_{k'=0}^{k}\binom{k}{k'}\pi_\mathrm{na}^{k'}u_\mathrm{a}^{k'}(1-\pi_\mathrm{na})^{k-k'}u_0^{k-k'}\,, \quad (8)$$

$$u_\mathrm{a}(k) = \sum_{k'=0}^{k}\binom{k}{k'}\pi_\mathrm{aa}^{k'}(1-\pi_\mathrm{aa})^{k-k'}u_0^{k-k'}\,. \quad (9)$$

The self-consistency equations can then be written as:

$$u_0 = g_1\,(\;(1-\pi_\mathrm{na})u_0 + \pi_\mathrm{na}u_\mathrm{a}\;)\,, \quad (10)$$
$$u_\mathrm{a} = g_1\,(\;p_\mathrm{app}((1-\pi_\mathrm{aa})u_0 + \pi_\mathrm{aa}) + (1-p_\mathrm{app})((1-\pi_\mathrm{aa})u_0 + \pi_\mathrm{aa}u_\mathrm{a})\;)\,, \quad (11)$$

and

$$s = 1 - (1-\pi_\mathrm{a})g_0\left((1-\pi_\mathrm{na})u_0 + \pi_\mathrm{na}u_\mathrm{a}\right) - \pi_\mathrm{a}g_0(\;p_\mathrm{app}((1-\pi_\mathrm{aa})u_0 + \pi_\mathrm{aa}) + (1-p_\mathrm{app})((1-\pi_\mathrm{aa})u_0 + \pi_\mathrm{aa}u_\mathrm{a}))\,, \quad (12)$$

where g_0 and g_1 are, respectively, the generating functions for degree and extended degree distributions [46], p_app is the probability the app work as expected ($1-p_\mathrm{app}$ is then the probability that the app-user does not quarantine her/himself after being notified of exposure to an infectious app-user) and s is the fraction of nodes infected through non-app-users. Note that π_na is determined by the free parameters π_a and π_aa as we already showed that $\pi_\mathrm{na} = \frac{\pi_\mathrm{a}}{1-\pi_\mathrm{a}}(1-\pi_\mathrm{aa})$. When $\pi_\mathrm{aa} = \pi_\mathrm{a}$ we can write the relative extended component size s' which also includes individuals caught infection though an app-user before s/he could quarantine her/himself (see Sec. II C 1) as

$$s' = s + (1-s)(1-\mathrm{e}^{-s\pi_\mathrm{a}^2 qpp_\mathrm{app}})\,, \quad (13)$$

where q is the expected excess degree.

In the case of including a transmission probability p which is less than 1 (in the above equations it was assumed the links are transmitting with probability 1), Eqs. 10 and 11 will change to:

$$u_0 = 1 - p + pg_1((1-\pi_\mathrm{na})u_0 + \pi_\mathrm{na}u_\mathrm{a})\,, \quad (14)$$
$$u_\mathrm{a} = 1 - p + pg_1((1-p_\mathrm{app})((1-\pi_\mathrm{aa})u_0 + \pi_\mathrm{aa}u_\mathrm{a}) + p_\mathrm{app}((1-\pi_\mathrm{aa})u_0 + \pi_\mathrm{aa}))\,. \quad (15)$$

When the fraction $\pi_{\rm a}$ of nodes selected to adopt the app are all the highest degree nodes in the network, a fraction $\eta_{\rm a}$ of the links are protruding from the app-users (which are the top $\pi_{\rm a}$ fraction of nodes). These nodes all have a degree higher than $k_{\rm a}-1$ such that they include some of $k_{\rm a}$ nodes and the rest are comprised of all nodes with degree larger than $k_{\rm a}$. Then we can write $\eta_{\rm a}$ as:

$$\eta_{\rm a} = r^* k_{\rm a} p_{k_{\rm a}}/\langle k\rangle \sum_{k_{\rm a}+1}^{\infty} k p_k/\langle k\rangle \tag{16}$$

$$= \sum_{k_{\rm a,right}}^{\infty} k p_k/\langle k\rangle\,, \tag{17}$$

where r^* is the fraction of degree $k_{\rm a}$ nodes that are app-users and in Eq. 17 we absorbed r^* into p_k so that $p_{k_{\rm a,right}} = r^* k_{\rm a} p_{k_{\rm a}}$ represents the fraction of nodes in the network that have degree $k_{\rm a}$ and are app-users (so in Eq. 17, $k_{\rm a,right}$ takes the value $k_{\rm a}$).

Then for a network with homo/heterophily:

$$u_0 = 1-p+p\frac{1}{1-\eta_{\rm a}}\sum_{k=0}^{k_{\rm a,left}} q_k\left[(1-\pi_{\rm na})u_0+\pi_{\rm na}u_{\rm a}\right]^k\,, \tag{18}$$

$$u_{\rm a} = 1-p+p\frac{1}{\eta_{\rm a}}\sum_{k_{\rm a,right}}^{\infty} q_k[(1-p_{\rm app})((1-\pi_{\rm aa})u_0+\pi_{\rm aa}u_{\rm a}) + p_{\rm app}((1-\pi_{\rm aa})u_0+\pi_{\rm aa})]^k\,, \tag{19}$$

and

$$s = 1-\sum_{k=0}^{k_{\rm a,left}} p_k\left[(1-\pi_{\rm na})u_0+\pi_{\rm na}u_{\rm a}\right]^k - \sum_{k_{\rm a,right}}^{\infty} p_k[(1-p_{\rm app})((1-\pi_{\rm aa})u_0+\pi_{\rm aa}u_{\rm a}) + p_{\rm app}((1-\pi_{\rm aa})u_0+\pi_{\rm aa})]^k\,. \tag{20}$$

a special case of which are networks with neutral (non-existing) homophily, where $\pi_{\rm aa}$ is obtained to be equal to $\eta_{\rm a}$ and accordingly $\pi_{\rm na}=\eta_{\rm a}$, therefore,

$$u_0 = 1-p+p\frac{1}{1-\eta_{\rm a}}\sum_{k=0}^{k_{\rm a,left}} q_k\left[(1-\eta_{\rm a})u_0+\eta_{\rm a}u_{\rm a}\right]^k\,, \tag{21}$$

$$u_{\rm a} = 1-p+p\frac{1}{\eta_{\rm a}}\sum_{k_{\rm a,right}}^{\infty} q_k[(1-p_{\rm app})((1-\eta_{\rm a})u_0+\eta_{\rm a}u_{\rm a}) + p_{\rm app}((1-\eta_{\rm a})u_0+\eta_{\rm a})]^k\,, \tag{22}$$

and

$$s = 1-\sum_{k=0}^{k_{\rm a,left}} p_k\left[(1-\eta_{\rm a})u_0+\eta_{\rm a}u_{\rm a}\right]^k - \sum_{k_{\rm a,right}}^{\infty} p_k[(1-p_{\rm app})((1-\eta_{\rm a})u_0+\eta_{\rm a}u_{\rm a}) + p_{\rm app}((1-\eta_{\rm a})u_0+\eta_{\rm a})]^k\,. \tag{23}$$

These results predict the behavior of the epidemic dynamics in the thermodynamic limit, therefore they describe the dynamics very well when the network size is large enough.

C. Component size simulations

Next, we describe the way to extract the giant component in simulated networks and how these simulation results can be used for finding the critical points of the disease spreading process. The component sizes can also be used to find the epidemic size distributions as described in Section I B.

1. *Component Extension*

In each simulation run, we simulate one network structure G and distribute the apps to the nodes according to one of the models described in Section I C. From the original network G, we keep each link with probability $p = 1-e^{-\beta\tau}$, which is the probability of infection going through a link without apps. We also remove all the links between two app-users with probability $p_{\rm app}$ and call the resulting network $G_{\rm a}$. The components of graph $G_{\rm a}$ are the normal components.

The extended components can be reached by going through every normal component and extending it. For every app-user in the component $\alpha\in C$, we go through the neighbors $n_\alpha = \{\alpha_1,\alpha_2,,...,\alpha_k\}$ in the original network G. If α_i is an app-user and not in the component $\alpha_i\notin C$, we add it to the component extension C' with probability p. The total set of infected nodes, if starting from a node in C, is going to be $C\cup C'$. As these are disjoint sets, we can compute the size as $S'_C = |C|+|C'|$ and $S_{\rm c} = |C|$.

2. *Susceptibility*

In numerical simulations of finite size systems we can use the peak of a susceptibility measure to find the critical transition point. Theoretically, susceptibility [46] is a measure of fluctuation in the component sizes which is singular at the epidemic threshold (the critical point). In network percolation studies, it is defined as the expected growth in the size of the giant component when a random link is added to the network. Therefore, susceptibility in an ordinary percolation problem can be written as:

$$\chi = \frac{\sum_{c\neq c_{\rm max}} S_c^2 - S_{c_{\rm max}}^2}{N - S_{c_{\rm max}}}\,, \tag{24}$$

where S_c is the size of the component c, $c_{\rm max} = {\rm argmax_c S_c}$ is the largest component.

This formulation of susceptibility is not suitable in the current case. In fact, using the maximum value of Eq. 24

could lead to estimates of critical points that are very far from the actual one. Instead, we want to compute the expected growth in the extended giant component, which can be computed as:

$$\chi' = \frac{\sum_{c \neq c_{\max}} S_c S'_c (1 - \frac{S'_{c_{\max}}}{N})}{N - S_{c_{\max}}}, \qquad (25)$$

where S_c and S'_c are the size and the extended size of the component c and $c_{\max} = \text{argmax}_c S'_c$ is the largest component measured in the extended size.

III. NUMERICAL RESULTS

We will next illustrate using the theory and simulation introduced in Sec. II how the various parameters affect the epidemic sizes and epidemic probabilities. The simulation studies are done in networks of 10^4 nodes and averaged over 10 realizations. We use two network topologies: homogeneous networks (Erdős-Rényi networks) with expected degree $\langle k \rangle = 10$ and networks created with the configuration model with power-law degree distribution $p(k) = k^{-3}$, where the amount of degree 1 nodes is adjusted such that the average degree is 10. We then vary the effective degree $\bar{k} = p\langle k \rangle$ by randomly removing links from these initial networks.

A. Differences in normal and extended components

The difference of the epidemic probability (normal component size) and the epidemic size (extended component size), is a phenomenon that is specific to epidemics in the presence of app-adaptors. Breaking the equivalence of these two measures can have practical consequences as illustrated in Fig. 2a. The difference between these two grows with the fraction of app-users π_a. For example, when $\pi_a = 0.8$ and the epidemic probability (the normal component size) is $s_{\max} \approx 0.5$, the epidemic size (the extended component size) reaches $s_{\max} \approx 0.8$. This is reflected also in the expected epidemic sizes (see Fig. 2b). Despite the two component definitions differing from each other, they still display the transition at the same point and this point can be measured numerically using the susceptibilities defined in Eqs. (24)-(25) (see Fig. 2c).

The extended component size is not a conserved quantity like the normal component size in the sense that the sum of component sizes $S_\sum$ would always sum to the number of nodes N. Instead, the sum of component sizes can be significantly larger than the number of nodes (see Fig. 2d) and the maximum value it can reach grows with the number of application users π_a. The deviation from $S_\sum/N = 1$ reaches its maximum with disease parameters higher than the threshold values, but when the disease reaches a large enough population the fraction $S_\sum/N$ starts to decay reaching $S_\sum/N = 1$ when everybody belongs to the normal giant component.

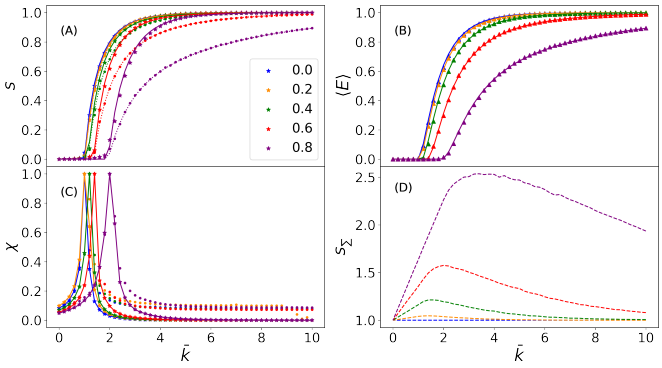

FIG. 2. Disease spreading statistics in an Erdős-Rényi network as a function of the effective degree $\bar{k}$ when there are π_a applications that are distributed uniformly randomly. Results are normalised to the network size N and shown for $\pi_a \in [0, 0.2, 0.4, 0.6, 0.8]$. The lines indicate the results from theory introduced in Sec. II B and the markers are results computed from component sizes of simulated networks as described in Sec. II C. (a) The normal component size, i.e., the epidemic probability, (dotted lines and dots) and the extended components, i.e. the epidemic size, (solid lines and stars) (b) Expected size of the epidemic (lines and diamonds). (c) Susceptibility of the normal giant component χ (dots) and the extended component χ' (lines with stars). Picks are the same positions for both types of curves. (d) The fraction of sum of component sizes and network size $S_\sum/N$.

B. Quarantine failures

The assumption in Section III A is that i) apps work perfectly and ii) an app-user always self-isolates before having a chance to apps the infection, meaning that there are no quarantine failures, $p_{\text{app}} = 1$. It is of practical significance to investigate the effects of quarantine failures on the epidemic threshold and epidemic size. Fig. 3 shows that in the absence of major quarantine failures, epidemic tracing and mitigation with apps can still be a valid strategy if app adoption level in a society is high enough. The effect of app adoption rate π_a is more important than the rate at which apps function, but both need to be relatively high in order for the apps to have a significant impact.

Even if we are above the epidemic threshold, the apps can be useful. Especially when the application adoption π_a is high, the quarantines can be very unreliable and the outbreak size (Fig. 3b-c) and epidemic probability (Fig. 3d) both remain small. Again, overall both the app adoption and quarantine reliability are important, with the app adoption rate being more important.

C. Degree heterogeneity and high-degree app targeting

Real networks are degree-heterogeneous and this heterogeneity has a strong effect on the final outbreak size and the epidemic threshold. Fig. 4 shows the expected

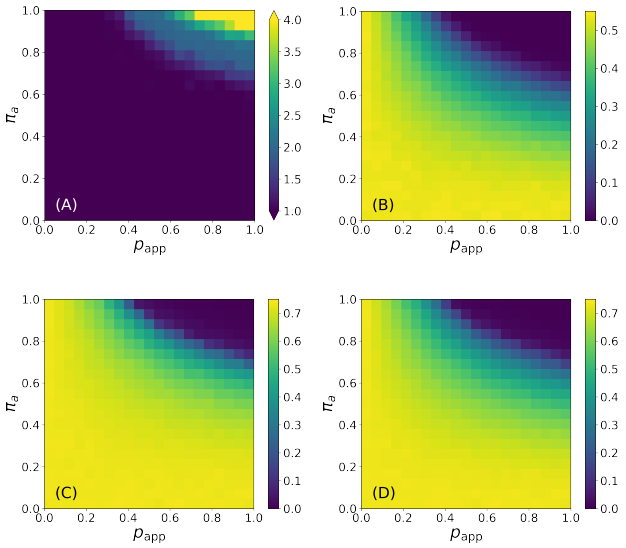

FIG. 3. The effect of quarantine failures in homogeneous network in which app adoption is done randomly. (a) The epidemic threshold as a function of quarantine probability p_{app} and app adoption rate π_{a}. All threshold values larger than 4 are shown with the same color. By setting the effective connectivity of the network to $\bar{k} = 1.8$ (b) the expected epidemic size, (c) the extended giant component size and (d) the normal giant component size are shown as a function of p_{app} and π_{a}.

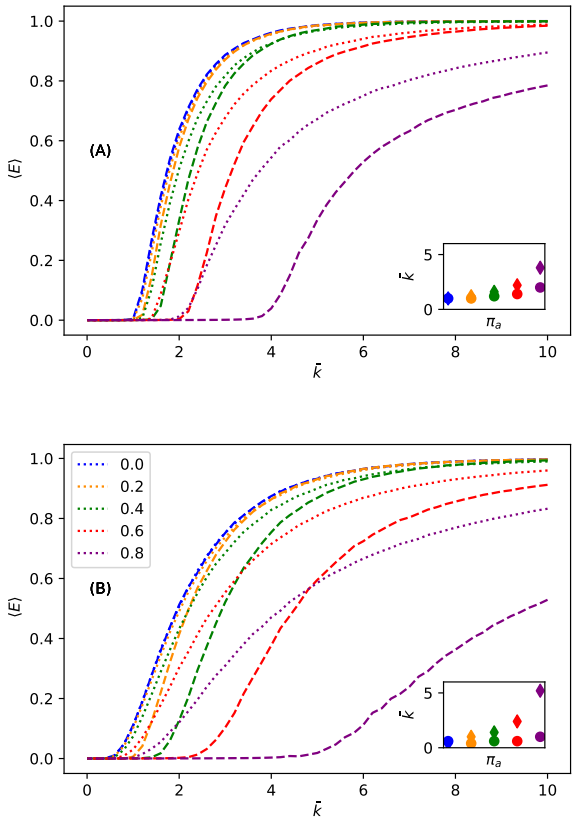

FIG. 4. Effects of contact tracing on the expected epidemic size and the epidemic threshold (insets) using two different strategies, random app adoption (small dots) and high-degree targeting (dotted lines) in (a) homogeneous networks with Poisson degree distribution and (b) heterogeneous networks with a power-law degree distribution $P(k) \propto k^{-3}$. Results are shown for $\pi_{\text{a}} \in [0, 0.2, 0.4, 0.6, 0.8]$.

epidemic sizes with two different strategies in app adoption, random and high-degree targeting for different fractions of app-users π_{a} in the network. In the homogeneous network, Fig. 4a, contact tracing decreases the expected epidemic size and pushes the epidemic threshold forward. These effects can be further amplified by shifting to the high-degree targeting in app adoption. With 80% of app-users, the epidemic threshold can move from $\bar{k} = 1$ to $\bar{k} = 4$ which means at that point expected epidemic size is zero while without contact tracing it would be almost 1. Note that in homogeneous networks, the effective average degree of the contact network $\bar{k}$, has a good correspondence to the reproduction number of the infection.

In networks with degree-heterogeneity, the epidemic threshold vanishes in normal SIR processes. This effect holds in contact-traced epidemics if distribute the apps uniformly randomly. However, from Fig. 4b it is clear that contact tracing can significantly reduce the expected epidemic size even when the apps are randomly distributed and the epidemic threshold remains unchanged. With a high-degree targeting strategy, it is possible to move the epidemic threshold. Comparing the expected epidemic size at different values of $\bar{k} < 3$ shows that in real-world situations, app adoption of super spreaders is of significant importance. Since hubs become the app-users, this strategy has drastic effects on the size and threshold of the epidemic, such that the threshold get pushed from somewhere near zero to some value $\bar{k} > 5$. Therefore, the reproduction number can be much more controlled in the high-degree targeting strategy.

D. The effect of homophily and heterophily

In previous sections, there was an assumption that app-users are disturbed with random mixing patterns: the fact that one of the connections of a node is an app-user has no effect on the probability of that node to be an app adopter. Next, we explore how homophily/heterophily affects the epidemics based on the app usage.

The Fig. 5 illustrates that increasing heterophily always leads to larger epidemics and lower epidemic threshold. Increasing homophily from random mixing is initially preferable, but the optimum lies between random mixing and full homophily. For the expected epidemic size, strong heterophily is especially detrimental (see Fig. 5a for the homogeneous network and with random

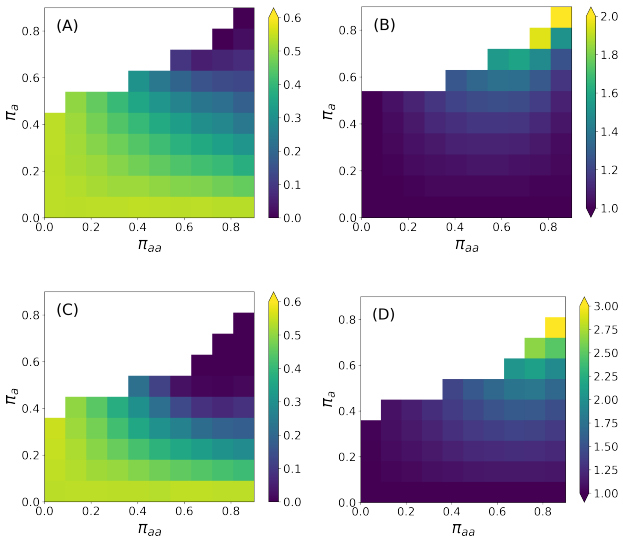

FIG. 5. The effect of homophily/heterophily in app adoption in homogeneous networks. Expected epidemic size at $\bar{k} = 1.8$ for (a) random app adoption and for (c) high-degree targeting strategy. Epidemic threshold for (b) random app adoption and for (d) the high-degree targeting strategy. Thresholds are from theoretical results and expected epidemic sizes are from percolation simulations. The empty white region is the spectrum that having such a homo/heterophilic population is impossible.

app adoption and in Fig. 5c for high-degree targeting strategy). The optimum value for heterophily/homophily is especially visible for the epidemic thresholds in Fig. 5b and Fig. 5d, respectively, for the random and high-degree targeting strategies.

IV. DISCUSSIONS

We expand the framework of using consistency equations to analyze digital contact tracing [33], which is an alternative to other approaches [60]. Contrary to the conventional SIR spreading, a full picture of the late-state epidemics in the presence of digital contact tracing is not given by a single observable (the component size) but one also needs two variables (normal and extended component sizes). These correspond to the probability of the epidemic and the epidemic size, which are equivalent in the SIR process. Here we see that the two quantities can be significantly different if the number of application users is high.

Our numerical work illustrates that the results of digital contact tracing can be very sensitive to the network structure, how applications are distributed among the population and how well the tracing works. That is, realistic estimates of the effects of digital contact tracing can only be achieved if one is able to choose correct parameter ranges in a high-dimensional parameter space. In this study, we had 6 of such parameters: shape of the degree distribution, average degree, amount of heterophily/homophily, application prevalence, quarantine probability and targeting strategy. While we were able to establish and confirm basic laws governing individual parameters and some combinations of parameters, exploring such a parameter space fully for possible compound effects is out of the reach. However, these types of effects can be largely revealed by inspecting the analytic equations we derived.

There are of course several open questions for which the results are only hinted by this study and other studies. Clearly, there are types of network structures we ignore here. For example, the heterophily and homophily could be constructed in the network in slightly different ways. From a practical point of view, one could create networks based on real age-based contact structures and digital contact tracing prevalence and estimate the benefits of applications relative to the risk groups.

Overall the problem of digital contact tracing offers not only a practical problem to solve, but an interesting theoretical puzzle, because it introduces memory to the epidemic process. This memory is limited to one step within the tracing model we use here, but one could also use multi-step tracing, where also the second neighbors of infected nodes are quarantined in the case that the first neighbors have already passed on the infection. Further, here we ignore effects such as quarantines that do not directly stop the infection from one application user to another from spreading further. However, in the case that there is a strong group structure in the network, there could be for example situations where a non-application user A infects application user B who alerts another application user C, who actually gets infected by A and stops the spreading because of the quarantine. Analyzing such more complicated phenomena can provide challenges for network scientists for years to come.

ACKNOWLEDGEMENT

The simulations presented above were performed using computer resources within the Aalto University School of Science “Science-IT” project. AF acknowledges funding by Science Foundation Ireland Grant No. 16/IA/4470, No. 16/RC/3918, No. 12/RC/2289P2 and No. 18/CRT/6049.

[1] N. Perra, Non-pharmaceutical interventions during the covid-19 pandemic: A review, Physics Reports https://doi.org/10.1016/j.physrep.2021.02.001 (2021).

[2] M. J. Keeling and P. Rohani, *Modeling infectious diseases in humans and animals* (Princeton university press, 2011).

[3] W. H. Foege, J. D. Millar, and J. M. Lane, Selective epidemiologic control in smallpox eradication, American journal of epidemiology **94**, 311 (1971).

[4] K. C. Swanson, C. Altare, C. S. Wesseh, T. Nyenswah, T. Ahmed, N. Eyal, E. L. Hamblion, J. Lessler, D. H. Peters, and M. Altmann, Contact tracing performance during the ebola epidemic in liberia, 2014-2015, PLoS neglected tropical diseases **12**, e0006762 (2018).

[5] G. W. Rutherford and J. M. Woo, Contact tracing and the control of human immunodeficiency virus infection, JAMA **259**, 3609 (1988).

[6] G. J. Fox, S. E. Barry, W. J. Britton, and G. B. Marks, Contact investigation for tuberculosis: a systematic review and meta-analysis, European Respiratory Journal **41**, 140 (2013).

[7] A. Aleta, D. Martin-Corral, A. P. y Piontti, M. Ajelli, M. Litvinova, M. Chinazzi, N. E. Dean, M. E. Halloran, I. M. Longini Jr, S. Merler, *et al.*, Modelling the impact of testing, contact tracing and household quarantine on second waves of covid-19, Nature Human Behaviour **4**, 964 (2020).

[8] P. G. Walker, C. Whittaker, O. J. Watson, M. Baguelin, P. Winskill, A. Hamlet, B. A. Djafaara, Z. Cucunubá, D. O. Mesa, W. Green, *et al.*, The impact of covid-19 and strategies for mitigation and suppression in low-and middle-income countries, Science **369**, 413 (2020).

[9] S. M. Kissler, C. Tedijanto, E. Goldstein, Y. H. Grad, and M. Lipsitch, Projecting the transmission dynamics of sars-cov-2 through the postpandemic period, Science **368**, 860 (2020).

[10] J. Bell, G. Bianconi, D. Butler, J. Crowcroft, P. C. Davies, C. Hicks, H. Kim, I. Z. Kiss, F. Di Lauro, C. Maple, *et al.*, Beyond covid-19: network science and sustainable exit strategies, Journal of Physics: Complexity **2**, 021001 (2021).

[11] M. Gilbert, M. Dewatripont, E. Muraille, J.-P. Platteau, and M. Goldman, Preparing for a responsible lockdown exit strategy, Nature medicine **26**, 643 (2020).

[12] N. E. Kogan, L. Clemente, P. Liautaud, J. Kaashoek, N. B. Link, A. T. Nguyen, F. S. Lu, P. Huybers, B. Resch, C. Havas, A. Petutschnig, J. Davis, M. Chinazzi, B. Mustafa, W. P. Hanage, A. Vespignani, and M. Santillana, An early warning approach to monitor covid-19 activity with multiple digital traces in near real time, Science Advances **7**, 10.1126/sciadv.abd6989 (2021).

[13] S. Kojaku, L. Hébert-Dufresne, E. Mones, S. Lehmann, and Y.-Y. Ahn, The effectiveness of backward contact tracing in networks, Nature Physics , 1 (2021).

[14] M. Salathe, L. Bengtsson, T. J. Bodnar, D. D. Brewer, J. S. Brownstein, C. Buckee, E. M. Campbell, C. Cattuto, S. Khandelwal, P. L. Mabry, *et al.*, Digital epidemiology, PLoS Comput Biol **8**, e1002616 (2012).

[15] A. Natarajan, H.-W. Su, and C. Heneghan, Assessment of physiological signs associated with covid-19 measured using wearable devices, NPJ digital medicine **3**, 1 (2020).

[16] D. R. Seshadri, E. V. Davies, E. R. Harlow, J. J. Hsu, S. C. Knighton, T. A. Walker, J. E. Voos, and C. K. Drummond, Wearable sensors for covid-19: a call to action to harness our digital infrastructure for remote patient monitoring and virtual assessments, Frontiers in Digital Health **2**, 8 (2020).

[17] D. P. Oran and E. J. Topol, Prevalence of asymptomatic sars-cov-2 infection: a narrative review, Annals of internal medicine **173**, 362 (2020).

[18] E. Morales-Narváez and C. Dincer, The impact of biosensing in a pandemic outbreak: Covid-19, Biosensors and Bioelectronics **163**, 112274 (2020).

[19] G. Quer, J. M. Radin, M. Gadaleta, K. Baca-Motes, L. Ariniello, E. Ramos, V. Kheterpal, E. J. Topol, and S. R. Steinhubl, Wearable sensor data and self-reported symptoms for covid-19 detection, Nature Medicine **27**, 73 (2021).

[20] T. Mishra, M. Wang, A. A. Metwally, G. K. Bogu, A. W. Brooks, A. Bahmani, A. Alavi, A. Celli, E. Higgs, O. Dagan-Rosenfeld, *et al.*, Pre-symptomatic detection of covid-19 from smartwatch data, Nature Biomedical Engineering **4**, 1208 (2020).

[21] N. G. Becker, K. Glass, Z. Li, and G. K. Aldis, Controlling emerging infectious diseases like sars, Mathematical biosciences **193**, 205 (2005).

[22] M. Eichner, Case isolation and contact tracing can prevent the spread of smallpox, American journal of epidemiology **158**, 118 (2003).

[23] K. T. Eames and M. J. Keeling, Contact tracing and disease control, Proceedings of the Royal Society of London. Series B: Biological Sciences **270**, 2565 (2003).

[24] I. Z. Kiss, D. M. Green, and R. R. Kao, Infectious disease control using contact tracing in random and scale-free networks, Journal of The Royal Society Interface **3**, 55 (2006).

[25] R. M. HOWELL, W. J. Kassler, and A. Haddix, Partner notification to prevent pelvic inflammatory disease in women: cost-effectiveness of two strategies, Sexually transmitted diseases **24**, 287 (1997).

[26] C. Fraser, S. Riley, R. M. Anderson, and N. M. Ferguson, Factors that make an infectious disease outbreak controllable, Proceedings of the National Academy of Sciences **101**, 6146 (2004).

[27] M. Kretzschmar, Y. T. van Duynhoven, and A. J. Severijnen, Modeling prevention strategies for gonorrhea and chlamydia using stochastic network simulations, American Journal of Epidemiology **144**, 306 (1996).

[28] D. Klinkenberg, C. Fraser, and H. Heesterbeek, The effectiveness of contact tracing in emerging epidemics, PloS one **1**, e12 (2006).

[29] R. Huerta and L. S. Tsimring, Contact tracing and epidemics control in social networks, Phys. Rev. E **66**, 056115 (2002).

[30] P. Rodríguez, S. Graña, E. E. Alvarez-León, M. Battaglini, F. J. Darias, M. A. Hernán, R. López, P. Llaneza, M. C. Martín, O. Ramirez-Rubio, *et al.*, A population-based controlled experiment assessing the epidemiological impact of digital contact tracing, Nature communications **12**, 1 (2021).

[31] I. Braithwaite, T. Callender, M. Bullock, and R. W. Aldridge, Automated and partly automated contact tracing: a systematic review to inform the control of covid-19, The Lancet Digital Health (2020).

[32] M. Salathé, C. L. Althaus, N. Anderegg, D. Antonioli, T. Ballouz, E. Bugnion, S. Capkun, D. Jackson, S.-I. Kim, J. Larus, *et al.*, Early evidence of effectiveness of digital contact tracing for sars-cov-2 in switzerland, medRxiv (2020).

[33] A. Barrat, C. Cattuto, M. Kivelä, S. Lehmann, and J. Saramäki, Effect of manual and digital contact tracing on covid-19 outbreaks: a study on empirical contact data, medRxiv 10.1101/2020.07.24.20159947 (2020).

[34] E. Shim, A. Tariq, W. Choi, Y. Lee, and G. Chowell, Transmission potential and severity of covid-19 in south korea, International Journal of Infectious Diseases **93**, 339 (2020).

[35] J. Cohen and K. Kupferschmidt, Countries test tactics in 'war'against covid-19 (2020).

[36] G. Cencetti, G. Santin, A. Longa, E. Pigani, A. Barrat, C. Cattuto, S. Lehmann, M. Salathe, and B. Lepri, Digital proximity tracing on empirical contact networks for pandemic control, medRxiv , 2020 (2021).

[37] H. L. Hambridge, R. Kahn, and J.-P. Onnela, Examining sars-cov-2 interventions in residential colleges using an empirical network, medRxiv 10.1101/2021.03.09.21253198 (2021).

[38] R. Pastor-Satorras and A. Vespignani, *Evolution and structure of the Internet: A statistical physics approach* (Cambridge University Press, 2007).

[39] S. N. Dorogovtsev and J. F. Mendes, *Evolution of networks: From biological nets to the Internet and WWW* (OUP Oxford, 2013).

[40] R. Albert and A.-L. Barabási, Statistical mechanics of complex networks, Reviews of modern physics **74**, 47 (2002).

[41] R. Pastor-Satorras and A. Vespignani, Epidemic spreading in scale-free networks, Physical review letters **86**, 3200 (2001).

[42] D. Centola, An experimental study of homophily in the adoption of health behavior, Science **334**, 1269 (2011).

[43] S. Funk, M. Salathé, and V. A. Jansen, Modelling the influence of human behaviour on the spread of infectious diseases: a review, Journal of the Royal Society Interface **7**, 1247 (2010).

[44] V. von Wyl, M. Höglinger, C. Sieber, M. Kaufmann, A. Moser, M. Serra-Burriel, T. Ballouz, D. Menges, A. Frei, and M. A. Puhan, Drivers of acceptance of covid-19 proximity tracing apps in switzerland: panel survey analysis, JMIR public health and surveillance **7**, e25701 (2021).

[45] J. A. M. López, B. A. García, P. Bentkowski, L. Bioglio, F. Pinotti, P.-Y. Boëlle, A. Barrat, V. Colizza, and C. Poletto, Anatomy of digital contact tracing: role of age, transmission setting, adoption and case detection, Science Advances , eabd8750 (2021).

[46] M. Newman, *Networks* (Oxford university press, 2018).

[47] L. Hébert-Dufresne, B. M. Althouse, S. V. Scarpino, and A. Allard, Beyond r 0: heterogeneity in secondary infections and probabilistic epidemic forecasting, Journal of the Royal Society Interface **17**, 20200393 (2020).

[48] M. Boguná, R. Pastor-Satorras, and A. Vespignani, Absence of epidemic threshold in scale-free networks with degree correlations, Physical review letters **90**, 028701 (2003).

[49] M. Barthélemy, A. Barrat, R. Pastor-Satorras, and A. Vespignani, Velocity and hierarchical spread of epidemic outbreaks in scale-free networks, Physical review letters **92**, 178701 (2004).

[50] R. Pastor-Satorras and A. Vespignani, Epidemic dynamics in finite size scale-free networks, Physical Review E **65**, 035108 (2002).

[51] S. Dhara, R. van der Hofstad, and J. S. van Leeuwaarden, Critical percolation on scale-free random graphs: new universality class for the configuration model, Communications in Mathematical Physics , 1 (2021).

[52] L. Ferretti, C. Wymant, M. Kendall, L. Zhao, A. Nurtay, L. Abeler-Dörner, M. Parker, D. Bonsall, and C. Fraser, Quantifying sars-cov-2 transmission suggests epidemic control with digital contact tracing, Science **368** (2020).

[53] Y. Liu, R. M. Eggo, and A. J. Kucharski, Secondary attack rate and superspreading events for sars-cov-2, The Lancet **395**, e47 (2020).

[54] Z. Shen, F. Ning, W. Zhou, X. He, C. Lin, D. P. Chin, Z. Zhu, and A. Schuchat, Superspreading sars events, beijing, 2003, Emerging infectious diseases **10**, 256 (2004).

[55] S. Clémençon, H. De Arazoza, F. Rossi, and V. C. Tran, A statistical network analysis of the hiv/aids epidemics in cuba, Social Network Analysis and Mining **5**, 1 (2015).

[56] J. O. Lloyd-Smith, S. J. Schreiber, P. E. Kopp, and W. M. Getz, Superspreading and the effect of individual variation on disease emergence, Nature **438**, 355 (2005).

[57] K. Kupferschmidt, Why do some covid-19 patients infect many others, whereas most don't spread the virus at all, Science **10** (2020).

[58] S. L. Feld, Why your friends have more friends than you do, American Journal of Sociology **96**, 1464 (1991).

[59] M. E. Newman, Threshold effects for two pathogens spreading on a network, Physical review letters **95**, 108701 (2005).

[60] G. Bianconi, H. Sun, G. Rapisardi, and A. Arenas, Message-passing approach to epidemic tracing and mitigation with apps, Physical Review Research **3**, L012014 (2021).

[61] I. Kryven and C. Stegehuis, Contact tracing in configuration models, Journal of Physics: Complexity **2**, 025004 (2021).

[62] A. Allard, C. Moore, S. V. Scarpino, B. M. Althouse, and L. Hébert-Dufresne, The role of directionality, heterogeneity and correlations in epidemic risk and spread, arXiv:2005.11283 (2020).

[63] R. B. Simões, I. Amaral, and S. Santos, Tracking the outbreak and far beyond: How are public authorities using mobile apps to control covid-19 pandemic, Multidisciplinary Perspectives of Communication in a Pandemic Context **1**, 166 (2021).

[64] M. Abueg, R. Hinch, N. Wu, L. Liu, W. J. Probert, A. Wu, P. Eastham, Y. Shafi, M. Rosencrantz, M. Dikovsky, *et al.*, Modeling the combined effect of digital exposure notification and non-pharmaceutical interventions on the covid-19 epidemic in washington state, medRxiv (2020).

[65] A. Bassolas, A. Santoro, S. Sousa, S. Rognone, and V. Nicosia, Optimising the mitigation of epidemic spreading through targeted adoption of contact tracing apps, arXiv:2102.13013 (2021).

[66] M. Kendall, L. Milsom, L. Abeler-Dörner, C. Wymant, L. Ferretti, M. Briers, C. Holmes, D. Bonsall, J. Abeler, and C. Fraser, Epidemiological changes on the isle of wight after the launch of the nhs test and trace programme: a preliminary analysis, The Lancet Digital Health **2**, e658 (2020).

[67] G. Burgio, B. Steinegger, G. Rapisardi, and A. Arenas, The impact of homophily on digital proximity tracing, arXiv:2103.00635 (2021).

[68] M. E. Newman, Spread of epidemic disease on networks, Physical review E **66**, 016128 (2002).
[69] R. Pastor-Satorras, C. Castellano, P. Van Mieghem, and A. Vespignani, Epidemic processes in complex networks, Reviews of modern physics **87**, 925 (2015).
[70] R. Albert, H. Jeong, and A.-L. Barabási, Error and attack tolerance of complex networks, nature **406**, 378 (2000).
[71] R. Cohen, K. Erez, D. Ben-Avraham, and S. Havlin, Resilience of the internet to random breakdowns, Physical review letters **85**, 4626 (2000).
[72] A. Barrat, M. Barthelemy, and A. Vespignani, *Dynamical processes on complex networks* (Cambridge university press, 2008).
[73] S. N. Dorogovtsev, A. V. Goltsev, and J. F. Mendes, Critical phenomena in complex networks, Reviews of Modern Physics **80**, 1275 (2008).
[74] L. Basnarkov, M. Mirchev, and L. Kocarev, Random walk with memory on complex networks, Physical Review E **102**, 042315 (2020).
[75] P. Shu, Effects of memory on information spreading in complex networks, in *2014 IEEE 17th International Conference on Computational Science and Engineering* (IEEE, 2014) pp. 554–556.
[76] B. Bollobás and B. Béla, *Random graphs*, 73 (Cambridge university press, 2001).
[77] J. P. Gleeson, Cascades on correlated and modular random networks, Phys. Rev. E **77**, 046117 (2008).